



Signature molecular changes in the skeletal muscle of hindlimb unloaded mice

Muhammad Azeem^{a,*}, Rizwan Qaisar^b, Asima Karim^b, Anu Ranade^b, Adel Elmoselhi^b

^a Department of Applied Physics and Astronomy, College of Sciences, University of Sharjah, 27272, Sharjah, United Arab Emirates

^b Department of Basic Medical Sciences, College of Medicine, University of Sharjah, 27272, Sharjah, United Arab Emirates

ARTICLE INFO

Keywords:

Raman spectroscopy
Molecular changes
Skeletal muscle
SR stress

ABSTRACT

Hind-limb unloaded (HU) mouse is a well-recognized model of muscle atrophy; however, the molecular changes in the skeletal muscle during unloading are poorly characterized. We have used Raman spectroscopy to evaluate the structure and behavior of signature molecules involved in regulating muscle structural and functional health. The Raman spectroscopic analysis of gastrocnemius muscles was compared between 16-18 weeks old HU c57Bl/6J mice and ground-based controls. The spectra showed that the signals for asparagine and glutamine were reduced in HU mice, possibly indicating increased catabolism. The peaks for hydroxyproline and proline were split, pointing towards molecular breakdown and reduced tendon repair. We also report a consistently increased intensity in $> 1300 \text{ cm}^{-1}$ range in the Raman spectra along with a shift towards higher frequencies in the HU mice, indicating activation of sarcoplasmic reticulum (SR) stress during HU.

1. Introduction

Mechanical unloading of the skeletal muscle leads to a rapid loss of the muscle mass and the strength, which worsens with increasing duration of unloading. This condition is relevant to a plethora of scenarios from prolonged bed rest due to stroke, chronic diseases and bone fractures [1] as well as spaceflights by the astronauts [2]. However, the search for an effective pharmacological therapy as a countermeasure remains elusive, partly because the molecular mechanisms of muscle detriment in unloading remain poorly understood. A detailed molecular mapping of the skeletal muscle in unloading conditions is required to design therapeutic drugs with specific molecular targets. Over the past three decades, several studies have investigated the molecular changes during muscle unloading [1–3]. However, a rigorous characterization of these changes has not been performed. The Raman spectroscopy offers a unique non-biological approach to obtain a snapshot of global molecular changes in skeletal muscle during mechanical unloading.

The Raman spectroscopy has effectively been applied to the biological tissues [4–8], including for cancer diagnosis [9,10]. The characteristic peaks in the spectroscopic data of the biological samples are associated with the vibrational frequencies of certain molecules in the sample. However, the interpretations of the spectra in the literature are not consistent, partly because of variations in sample storage and

preparation as well as the type of the techniques [6,9] used.

In particular, the intrinsic flexibility of the biological molecules makes the interpretations of the Raman spectra more challenging. For example, the protein molecules in the biological tissues are dynamic, adopting different spatial structures and geometries in various conditions. Each geometrical configuration of a molecule has its own unique vibrational fingerprint, and the actual spectrum is the total of the fingerprints of all spatial molecular variants of a molecule. In addition, a certain low-energy molecular configuration is more stable than a high-energy one, which implies that not all the variants of a molecule are equally represented in a spectrum. This structural variation poses a significant problem for the characterization of the molecules through spectroscopic techniques.

In this work, we have attempted to overcome these problems to characterize the preferential molecular changes in the skeletal muscles under unloading conditions using the HU mouse model. First important parameter in the Raman spectroscopic experiments involving biological tissues is the choice of a laser of an appropriate wavelength. Due to phonon-photon interaction, the Raman signal is inherently very weak. Further, the Raman scattering intensity is inversely proportional to the 4th order of the illuminating wavelength implying that at the longer wavelengths, the intensity of the Raman signals would drop dramatically. Therefore, the Raman signals will be suppressed by the higher

* Corresponding author.

E-mail address: mazeem@sharjah.ac.ae (M. Azeem).

<https://doi.org/10.1016/j.bbrep.2021.100930>

Received 9 December 2020; Received in revised form 11 January 2021; Accepted 19 January 2021

2405-5808/© 2021 The Authors. Published by Elsevier B.V. This is an open access article under the CC BY-NC-ND license

(<http://creativecommons.org/licenses/by-nc-nd/4.0/>).

noise level and the decreased sensitivity if obtained by the illuminating sources of wavelengths higher than 800 nm. This has been the case with several previous studies [9] where the spectra was obtained by using 1064 nm wavelength source. Illumination by the shorter wavelength (405 nm or 532 nm), on the other hand, causes the materials to fluoresce which hides the Raman peaks. Therefore, in this study, a laser of wavelength 785 nm is used which offers the best balance between the scattering efficiency and influence of fluorescence.

In addition, no smoothing is performed on the spectra in this study. Instead, the experimental spectra is fitted with the Lorentz model to resolve the Raman peaks. Finally, the spectra are collected on the fresh samples rather than making slides. Our experiments showed that the asparagine and glutamine are the major molecular constituents of the skeletal muscles and in evaluating the molecular phenotypes of their biological tissues, our findings unravel novel molecular changes in the skeletal muscle under unloading conditions.

2. Materials and methods

Male, c57BL/6J mice were maintained under pathogen-free conditions, housed 2–3 mice per cage (control) or one mouse per cage (unloaded) in a 12:12 (light: dark) cycle and provided with food and water *ad libitum*, as described elsewhere [11]. All mice were 16–18 weeks old at the start of the experiments. One group of mice was mechanically unloaded with hind limbs suspended in air, while the other group was kept as the ground-based controls for a similar duration for 15 days.

To assess the muscles function, grip strength was measured with a Digital Grip Strength meter equipped with a Hind Limb Pull Bar Assembly (Columbus Instruments, Columbus, OH). Mice were allowed to grip the metal grids of a grip meter with their paws and gently pulled backwards by their tail until they could no longer hold the grids. The peak grip strength observed in 5 trials was recorded in grams.

After the period of unloading, mice were euthanized via cervical dislocation. Gastrocnemius muscle tissues were collected from the control and unloaded mice (N = 4–5/group) and were immediately snap-frozen in liquid nitrogen for analysis via Raman Spectroscopy as shown schematically in Fig. 1.

The Raman spectra were obtained by using Renishaw in via Raman spectrometer. Three specimens were selected for the control and the

unloaded samples each and 10 spectra were collected from various locations of each muscle to obtain the average. In each recording, a site of a specimen was exposed to a 785 nm wavelength laser with a spot size of 50 μm and a laser power of 1%. The spectral range was from 100 cm^{-1} to 1700 cm^{-1} , the fingerprint region where the signature peaks from the biological molecules can be found. To avoid damage to the muscle tissues from the intensity of the laser, the spectra were collected at the intervals of 500 cm^{-1} and then stitched together to obtain the full spectrum. The acquisition time for an individual spectrum was 10 s.

3. Theory and calculations

The frequencies and the intensities of the spectra were fitted with the Lorentzian function to resolve peaks contributed by each molecule in the sample [12]. The Lorentzian peak function is defined as,

$$f(x) = \frac{H}{4\left(\frac{x-x_0}{W}\right)^2 + 1} \quad (1)$$

where x_0 , H and W are the peak position, the height of the peak and the full width half maximum (FWHM), respectively. The natural shape of a spectral line is Lorentzian, which has a sharp narrow peak with most of the intensity of the peak located in the tails extending to infinity as shown in the Fig. 2. The Lorentzian function resolves the scattered intensity into peaks. A cumulative spectrum (Fig. 3) is then calculated which shows the overall fingerprint of a sample. The uncertainty in the excitation response, the location of the energy level of the excited state of the molecule as well as the duration for which it remains in the excited state influence the width of the Lorentzian line. Due to the scattered nature of the experimental spectra, the uncertainty in the position of peaks produced by the Lorentz fit is up to $\pm 5 \text{ cm}^{-1}$. All the spectra were normalized with respect to the strongest peak.

Total RNA was extracted from gastrocnemius muscles using TRI reagent and the cDNA was prepared from 1 mg of the total RNA using iScript™ cDNA Synthesis kit (Bio-Rad, Hercules, CA, USA). 2.5 ng of cDNA samples were amplified using specific primers along with fast SYBR green master mix (Applied Biosystems, Grand Island, NY, USA), as described previously [13]. Quantification of genes involved in glutamine (glutamine synthase and glutamine dehydrogenase) and asparagine (asparaginase) metabolism, as well as cellular SR stress (GRP78, ATF4, CHOP and s-XBP-1) was performed. The data were analyzed using

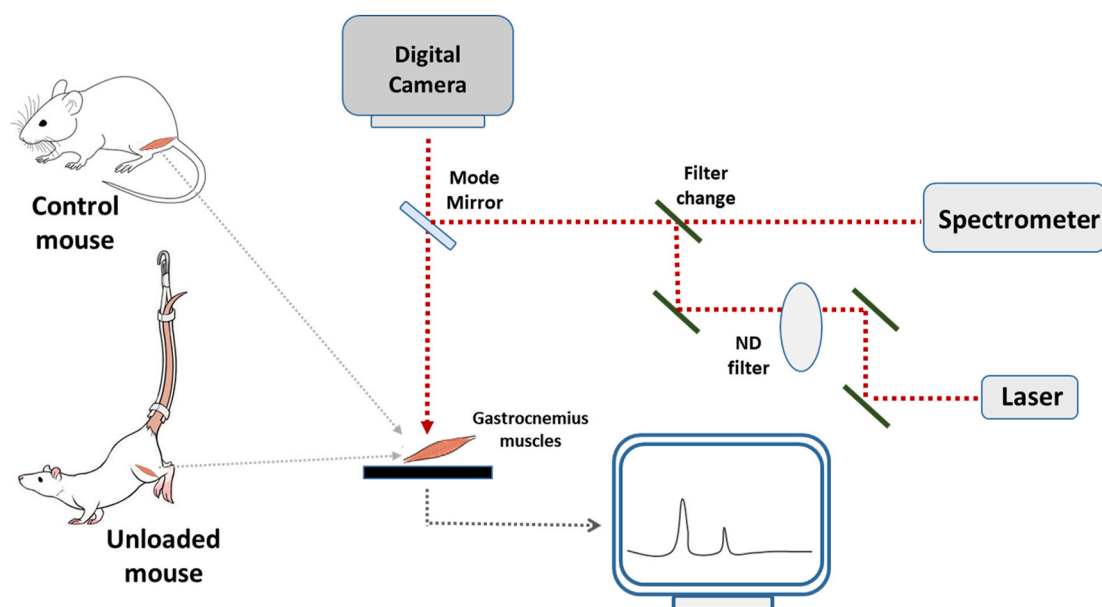


Fig. 1. Schematic representation of the experimental procedures. Gastrocnemius muscles were obtained from the hind-limb unloaded and ground-based control mice, and the Raman spectroscopic analysis was performed in the appropriate settings.

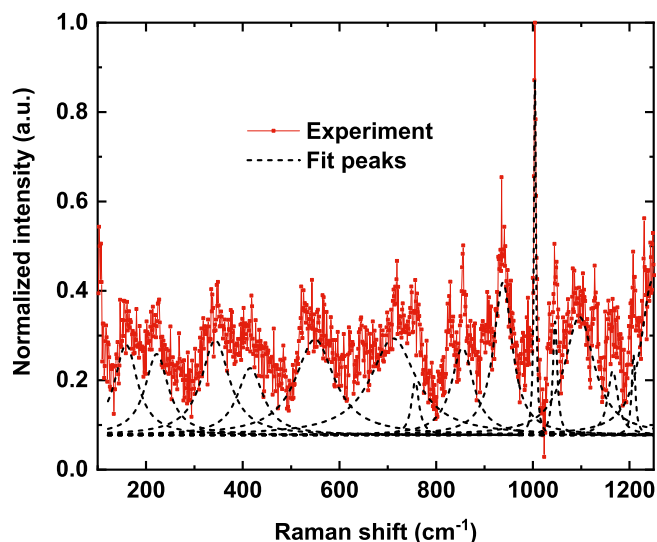


Fig. 2. Experimentally obtained Raman spectrum (red solid) and the fitted peaks (black dashed). Each peak is fitted with the Lorentz peak function. (For interpretation of the references to colour in this figure legend, the reader is referred to the Web version of this article.)

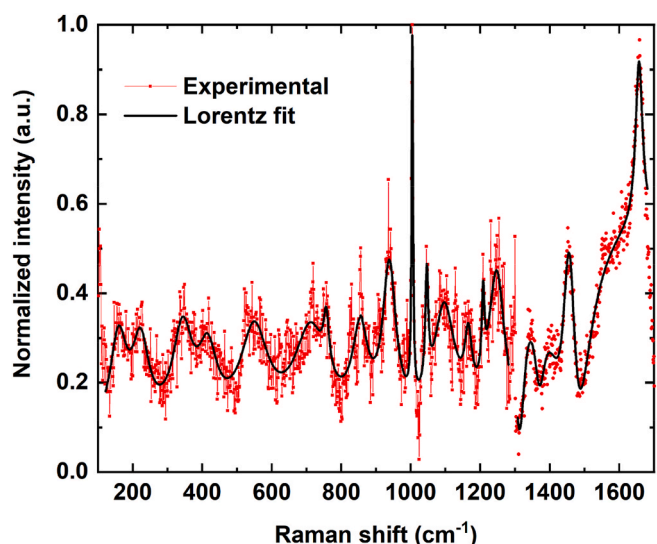


Fig. 3. The experimentally obtained Raman spectrum (red solid) of a control specimen along with a cumulative Lorentz fit (black solid). (For interpretation of the references to colour in this figure legend, the reader is referred to the Web version of this article.)

the $\Delta\Delta\text{Ct}$ method.

The data about muscle strength, mass and mRNA concentration is presented using mean and standard error of mean. Student's *t*-test was used for comparison between the two groups. A *p*-value < 0.05 was considered to be statistically significant. Statistical analysis was performed using GraphPad Prism version 8.

4. Results

The Raman spectra are the effect of the emission of the scattered light due to the change in the polarizability of the covalent bonds. Therefore, any signature changes registered in the control and unloaded samples can be read by the Raman spectroscopy. The Raman spectrum from a control sample is shown in Fig. 3 along with a Lorentz fit. The scattered spectrum indicates that the peaks contributed by the different molecules

overlap. The Lorentz fit, therefore, resolved the peaks more clearly to help identify the types and structures of the molecules as well as their vibrational modes.

By comparing our results with the previous studies [6,7,14], the bands at 159 cm^{-1} , 223 cm^{-1} , 344 cm^{-1} , and 1209 cm^{-1} were allocated to asparagine [14], whereas the bands from asparagine and glutamine overlapped at the frequencies 412 cm^{-1} , 533 cm^{-1} and 551 cm^{-1} . The peaks at 710 cm^{-1} and 755 cm^{-1} were due to the combined contributions of the hydroxyproline, UDP-D-glucose and tryptophan [7,9]. A peak at 1004 cm^{-1} is also assigned to the tryptophan molecule [6]. A contribution from the tyrosine molecule was at 595 cm^{-1} and the proline signature bands were at 936 cm^{-1} , 1046 cm^{-1} , 1090 cm^{-1} , 1125 cm^{-1} , 1166 cm^{-1} , and 1245 cm^{-1} . The bands at 1343 cm^{-1} and 1450 cm^{-1} were due to the twisting and bending of the CH₃ and CH₂ bonds of praline and proline molecules [6]. Similarly, shoulders at 1557 cm^{-1} and 1645 cm^{-1} were the signatures of carbon-carbon bond stretching in the praline molecule [6].

Next, we compared the Raman spectra of the control and unloaded samples as shown in Fig. 4. We found major differences in the positions and intensities of both the spectra, indicating qualitative and quantitative changes in the molecular cohorts constituting skeletal muscles. The peak at 159 cm^{-1} for the control sample is shifted to the lower frequency of at around 151 cm^{-1} in the unloaded sample, while the intensity of the peak at 220 cm^{-1} is slightly increased in the unloaded sample. The intensities of the unloaded sample at the 344 cm^{-1} and 412 cm^{-1} are significantly reduced compared to the control along with the appearance of a new peak at 460 cm^{-1} , indicating conformational changes in the asparagine and the glutamine molecules.

To elucidate the changes in Raman peaks of these amino acids, we measured the mRNA concentrations of the enzymes involved in their metabolism (Fig. 5B). Unloading resulted in significantly higher expressions of glutamine dehydrogenase, indicating increased catabolism of glutamine (Fig. 5B). We also found a trend, albeit not statistically significant, towards increase expression of asparaginase with unloading, indicating increased catabolism of asparagine. These findings, nevertheless do not rule out changes in activities of these enzymes. These amino acids are involved in regulating a variety of functions in the skeletal muscle including bioenergetics and protein synthesis [15]. Consequently, changes in their molecular orientation and/or relative proportions in the HU skeletal muscle can be potential contributors to the muscle atrophy and weakness in these mice.

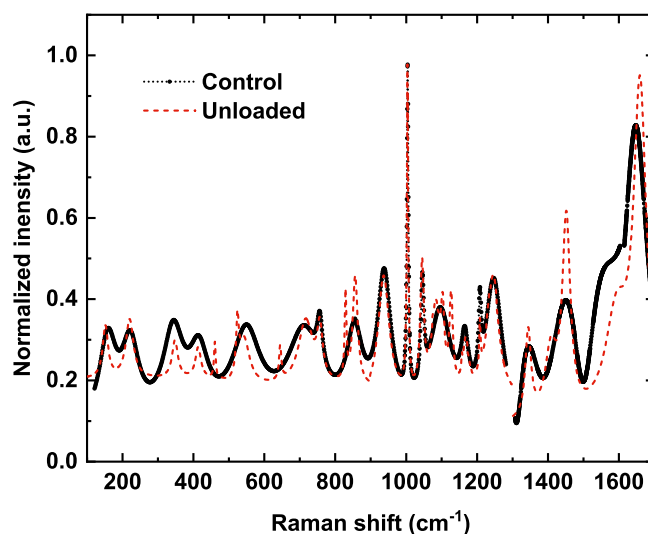


Fig. 4. Experimentally obtained Raman spectra from a control (black dotted) and unloaded specimen (red dashed). (For interpretation of the references to colour in this figure legend, the reader is referred to the Web version of this article.)

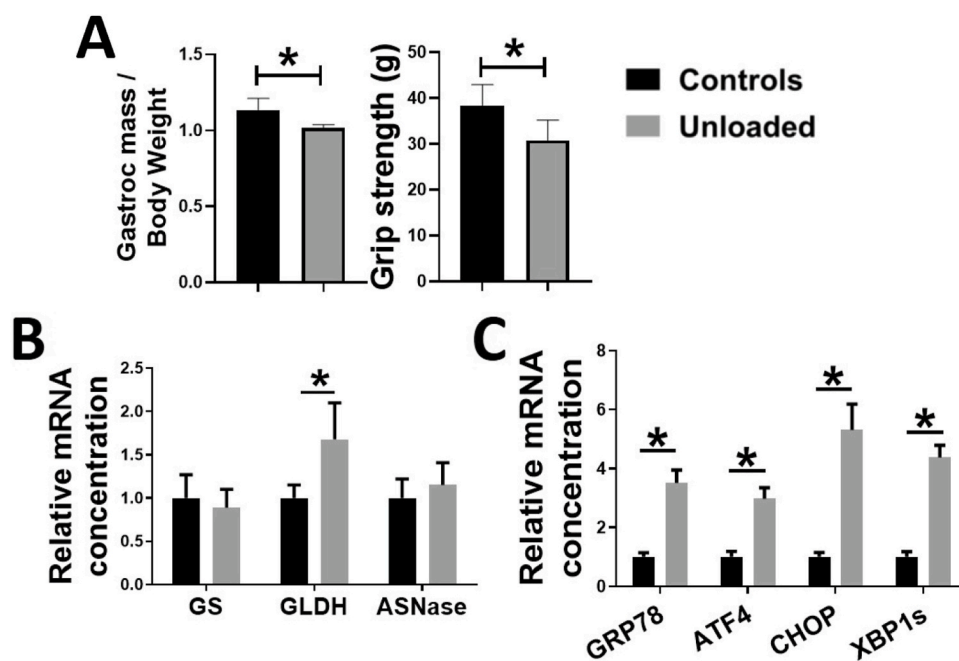


Fig. 5. The gastrocnemius muscle mass and grip strength in the control and unloaded mice (A) and the relative mRNA expressions of the enzymes involved in glutamine and asparagine metabolism (B) and the markers of SR stress (C) in gastrocnemius muscles of control and unloaded mice (GS; glutamine synthase, GLDH glutamine dehydrogenase, ASNase; asparaginase). (N = 5–8 per group), *p < 0.05.

We also found that the peak at 551 cm^{-1} was slightly shifted to the lower frequency of 525 cm^{-1} , with a shoulder appearing at 542 cm^{-1} for the asparagine and glutamine molecules. Additionally, a weak but sharp peak at 644 cm^{-1} appears in the unloaded samples, which was most probably due to hydroxyproline. The hydroxyproline is a derivative of proline and is a structural constituent of multiple muscle proteins. It is found in collagens in high concentrations and has a supportive role during muscle contraction [16,17]. Other hydroxyproline peak at 709 cm^{-1} was slightly shifted to a higher frequency of 717 cm^{-1} in the unloaded sample along with a small increase in the intensity whereas the peak at 756 cm^{-1} is unchanged. The changes in the height and displacement of the signature peak of hydroxyproline potentially means altered quality and/or quantity of this amino acid, which can have pathological consequences in the conditions of prolonged HU. The peak associated with tyrosine at 856 cm^{-1} was also split into two sharp and narrow peaks at 829 cm^{-1} and 857 cm^{-1} with higher intensity in the HU mice, when compared to control mice. Tyrosine is an alpha amino acid and plays an important role in the enzymatic activities of many proteins. Further, the proline peak at 1090 cm^{-1} was also split into three narrow peaks (triplet) at 1087 cm^{-1} , 1103 cm^{-1} and 1128 cm^{-1} . A doublet in the tyrosine and a triplet in the proline molecules suggests that some molecular residues in proteins undergo a change in their hydrogen bonding environment [18]. Thus, the changes in the tyrosine and proline can potentially contribute to the loss of muscle mass and/or strength in the unloading conditions.

The spectra above 1300 cm^{-1} showed some interesting findings. The spectral intensities of the unloaded muscles in this range were much stronger than the control muscles at all the positions with a shoulder forming at 1410 cm^{-1} . The intensity of the shoulder at 1557 cm^{-1} was significantly reduced and shifted to 1599 cm^{-1} for the unloaded samples. Similarly, the peak at 1645 cm^{-1} was also shifted to 1659 cm^{-1} .

5. Discussion

It is apparent that the unloaded samples have catabolic changes at the molecular level, with biological implications. The reduction in the Raman signal intensities from asparagine and glutamine indicate an

enhancement of the catabolic processes in unloaded muscle. The splitting of the hydroxyproline and proline peaks signifies the breakdown of these molecules, which is most likely associated with reduced healing and repair processes in the skeletal muscle during mechanical unloading. Similarly, a breakdown in the tyrosine molecules indicates reduced protein synthesis, which can potentially contribute to muscle atrophy and weakness. In accordance with the changes in Raman spectral analysis, we found significant reduction of the gastrocnemius muscle mass and grip force in HU mice, when compared with the control, in accordance with our previous findings (Fig. 5A) [11]. This can partly be due to the changes taking place in the frequency range of 100 cm^{-1} to 1300 cm^{-1} , according to the Raman spectra.

The changes in the spectral range greater than 1300 cm^{-1} have been attributed to the accumulation of unfolded protein in the sarcoplasmic reticulum (SR), a condition called SR stress [19]. In order to perform an independent validation of these findings, we conducted RT-PCR experiments as described previously [13]. Specifically, we quantified the signature mRNA markers of SR stress in the gastrocnemius muscles of control and unloaded mice. A significant upregulation in the mRNA expressions of GRP78, ATF4, CHOP and s-XBP-1 was reported in the unloaded mice (Fig. 5C), which indicate heightened SR stress and validates the Raman spectroscopic findings.

The SR stress is emerging as an important candidate process to the muscle decline during various catabolic conditions [20] and can potentially contribute to the loss of muscle mass and strength reported here in the HU mice. Thus, the perturbation of SR protein folding capacity, as indicated by changes in the spectral range $>1300\text{ cm}^{-1}$, seems a prime contributor to muscle detriment in the HU mice. The enhanced intensity of the Raman spectra in this range in the unloaded samples is also accompanied by a shift towards the higher frequency, a result of the broken molecules with shorter bond lengths, thus shifting the Raman peaks to the higher wave numbers. In addition, as described above, the spectra in the range of 1300 cm^{-1} to 1700 cm^{-1} are mainly the result of the CH₂, CH₃ vibrations; therefore, the higher intensity of the unloaded samples in this energy range was due to the accumulation of the broken molecules.

6. Conclusion

We have investigated the signature molecular changes in the skeletal muscles of the HU mice by using the Raman spectrometer. We conclusively show that the muscle atrophy and weakness in the unloaded samples are associated with the significant changes in the molecular phenotypes of skeletal muscle. Our key findings are the significant differences in the features of the Raman spectra between control and unloaded mouse muscles. The major components of the skeletal muscles are asparagine, glutamine, hydroxyproline, DL tyrosine, UDP-D-glucose, proline, praline and tryptophan. The concentrations of the asparagine and the glutamine molecules were significantly changed in the unloaded muscles as evident by the reduction in the intensities of the Raman peaks at 344 cm^{-1} and 412 cm^{-1} . The peaks at 460 cm^{-1} , 525 cm^{-1} , 542 cm^{-1} and 551 cm^{-1} in the unloaded samples illustrate the conformational changes in these molecules. The signatures peaks of hydroxyproline were at 709 cm^{-1} and 756 cm^{-1} in the control muscles, while for the unloaded muscles, a new peak appears at 644 cm^{-1} indicating the breakdown of the molecular bonds in the hydroxyproline. Similarly, the splitting and the shifting was observed in the peaks associated with tyrosine and the proline molecules. The spectra from the control and unloaded samples was also clearly distinguishable in the spectral ranges greater than 1300 cm^{-1} indicative of heightened SR stress, which was independently validated by RT-PCR data.

Authors contribution

M. A. collected the experimental data from Raman spectrometer and wrote the manuscript. R. Q. prepared the samples, performed statistical analysis and collected RT-PCR data and wrote the parts of the manuscript. A. R., A. K., A. E and A. M. provided assistance to R. Q. in the sample's preparation and storage.

Declaration of competing interest

The work is supported by the Unit university of Sharjah (UOS) competitive research grant 1802143076.

Acknowledgement

Authors are thankful to Dr. Hussain Alawadhi of center of advanced materials research, UOS, to provide unlimited access to the spectrometers and to Ms. Zainab Ibrahim for taking care of the mice.

References

- [1] Y. Gao, Y. Arfat, H. Wang, N. Goswami, Muscle atrophy induced by mechanical unloading: mechanisms and potential countermeasures, *Front. Physiol.* 9 (2018) 235, <https://doi.org/10.3389/fphys.2018.00235>.
- [2] A. Karim, A. Moslehi, R. Qaisar, Muscle unloading: a comparison between spaceflight and ground-based models, *Acta Physiol.* 228 (2020), e13431, <https://doi.org/10.1111/apha.13431>.
- [3] J. Ochala, A.M. Gustafson, M.L. Diez, G. Renaud, M. Li, S. Aare, R. Qaisar, V. C. Banduseela, Y. Hedström, X. Tang, B. Dworkin, G.C. Ford, K.S. Nair, S. Perera, M. Gautel, L. Larsson, Preferential skeletal muscle myosin loss in response to mechanical silencing in a novel rat intensive care unit model: underlying mechanisms, *J. Physiol.* 589 (2011) 2007–2026, <https://doi.org/10.1111/jphysiol.2010.202044>.
- [4] E. Bicknell-Brown, K.G. Brown, Phase transitions in combined rabbit muscle sarcoplasmic reticulum lipids by Raman spectroscopy, *Biochem. Biophys. Res. Commun.* 122 (1984) 446–451, [https://doi.org/10.1016/0006-291X\(84\)90496-0](https://doi.org/10.1016/0006-291X(84)90496-0).
- [5] K.T. Yue, J.-P. Yang, C.L. Martin, D.L. Sloan, R.H. Callender, Raman spectroscopy of liver alcohol dehydrogenase, *Biochem. Biophys. Res. Commun.* 122 (1984) 225–229, [https://doi.org/10.1016/0006-291X\(84\)90463-7](https://doi.org/10.1016/0006-291X(84)90463-7).
- [6] N. Huang, M. Short, J. Zhao, H. Wang, H. Lui, M. Korbelik, H. Zeng, Full range characterization of the Raman spectra of organs in a murine model, *Optic Express* 19 (2011) 22892, <https://doi.org/10.1364/OE.19.022892>.
- [7] N.K. Afseth, V.H. Segtnan, J.P. Wold, Raman spectra of biological samples: a study of preprocessing methods, *Appl. Spectrosc.* 60 (2006) 1358–1367, <https://doi.org/10.1366/000370206779321454>.
- [8] E.B. Hanlon, R. Manoharan, T.W. Koo, K.E. Shafer, J.T. Motz, M. Fitzmaurice, J. R. Kramer, I. Itzkan, R.R. Dasari, M.S. Feld, Prospects for in vivo Raman spectroscopy, *Phys. Med. Biol.* 45 (2000), <https://doi.org/10.1088/0031-9155/45/2/201>.
- [9] Z. Movasaghi, S. Rehman, I.U. Rehman, Raman spectroscopy of biological tissues, *Appl. Spectrosc. Rev.* 42 (2007) 493–541, <https://doi.org/10.1080/05704920701551530>.
- [10] R.K. Dukor, *Vibrational Spectroscopy in the Detection of Cancer*, 2006, <https://doi.org/10.1002/0470027320.s8107>, J.M. Chalmers and P.R. Griffiths.
- [11] M. Maffei, E. Longa, R. Qaisar, V. Agoni, J.F. Desaphy, D. Conte Camerino, R. Bottinelli, M. Canepari, Actin sliding velocity on pure myosin isoforms from hindlimb unloaded mice, *Acta Physiol.* 212 (2014) 316–329.
- [12] W.J. Hehre, *A Guide to Molecular Mechanics and Quantum Chemical Calculations*, Wavefunction, Inc. 18401 Von Karman Ave., Suite 370 Irvine, CA 92612, 2003.
- [13] N. Alamdari, G. Toraldo, Z. Aversa, I. Smith, E. Castellero, G. Renaud, R. Qaisar, L. Larsson, R. Jasuja, P.O. Hasselgren, Loss of muscle strength during sepsis is in part regulated by glucocorticoids and is associated with reduced muscle fiber stiffness, *Am. J. Physiol. Regul. Integr. Comp. Physiol.* 303 (2012), <https://doi.org/10.1152/ajpregu.00636.2011>.
- [14] B.O. Golichenko, Raman study of L-Asparagine and L-Glutamine molecules adsorbed on aluminum films in a wide frequency range, *Semicond. Phys. Quantum Electron. Optoelectron.* 20 (2017) 297–304, <https://doi.org/10.15407/spqe020.03.297>.
- [15] Y. Kamei, Y. Hatazawa, R. Uchitomi, R. Yoshimura, Regulation of skeletal muscle function by, *Nutrients* 12 (2020).
- [16] I.H. Koh, H.J. Kang, W.T. Oh, J.J. Hong, Y.R. Choi, Correlation between change in muscle excursion and collagen content after tendon rupture and delayed repair, *J. Orthop. Surg. Res.* 12 (2017) 1–7, <https://doi.org/10.1186/s13018-017-0518-y>.
- [17] B.F. Miller, J.L. Olesen, M. Hansen, S. Døssing, R.M. Cramer, R.J. Welling, H. Langberg, A. Flyvbjerg, M. Kjaer, J.A. Babraj, K. Smith, M.J. Rennie, Coordinated collagen and muscle protein synthesis in human patella tendon and quadriceps muscle after exercise, *J. Physiol.* 567 (2005) 1021–1033, <https://doi.org/10.1113/jphysiol.2005.093690>.
- [18] A. Mizuno, Y. Ozaki, K. Itoh, S. Matsushima, K. Iriyama, Raman spectroscopic evidence for the microenvironmental change of some tyrosine residues of lens proteins in cold cataract, *Biochem. Biophys. Res. Commun.* 119 (1984) 989–994, [https://doi.org/10.1016/0006-291X\(84\)90871-4](https://doi.org/10.1016/0006-291X(84)90871-4).
- [19] A. Hosoda, A. Maruyama, D. Oikawa, Y. Oshima, Y. Komachi, G. Kanai, H. Sato, T. Iwakaki, Detection of ER stress in vivo by Raman spectroscopy, *Biochem. Biophys. Res. Commun.* 405 (2011) 37–41, <https://doi.org/10.1016/j.bbrc.2010.12.112>.
- [20] D. Afroze, A. Kumar, ER stress in skeletal muscle remodeling and myopathies, *Physiol. Behav.* 176 (2016) 139–148, <https://doi.org/10.1016/j.physbeh.2017.03.040>.